

Sliding Mode Control for Stabilizing of Boost Converter in a Solid Oxide Fuel Cell

Junsheng Jiao

*School of Electronic Engineering, Tongling University, Tongling City, Anhui Province, China, 244061
Emails: jiaotlu@sina.com*

Abstract: *The output voltage of Solid Oxide Fuel Cell (SOFC) is usually changed with the temperature and hydrogen flow rate. Since the fuel cell can generate a wide range of voltages and currents at the terminals, as a consequence, a constant DC voltage and function cannot be maintained by itself as a DC voltage power supply source. To solve this problem, a simple SOFC electrochemical model is introduced to control the output voltage. The Sliding Mode Control (SMC) is used to control the output voltage of the DC-DC converter for maintaining the constant DC voltage when the temperature and hydrogen flow rate are changed. By the simulation results it can be seen that the SMC technique has improved the transient response and reduced the steady state error of DC voltage.*

Keywords: *Sliding mode control, DC-DC converter, solid oxide fuel cell, stabilization, model.*

1. Introduction

Now the batteries are widely used in all fields. However, fuel cell systems can provide an alternative power source relative to the traditional, combustion-based batteries [1]. And in general, the chemical energy is stored in batteries and the electrolyte converts it into electricity when needed until the chemical energy is depleted. Though the depleted secondary batteries can be recharged from an external power source, the primary batteries must be replaced [2]. The fuel cells do not store chemical energy, but rather convert the chemical energy of the fuel into electricity. Thus, the fuel cells do not need recharging and can continuously produce electricity as long as fuel and oxidant are supplied. Fuel cells combine higher fuel efficiency with low or no pollution, greater flexibility in installation and

operation, quiet operation, low vibration, and potentially lower maintenance and capital costs.

For the rapid response to varying load demands, low-temperature types, such as the Proton Exchange Membrane Fuel Cell (PEMFC) are suitable for automotive applications [3]. Then high-temperature types, such as the solid oxide fuel cell can be applied in stationary power generation systems due to their high-thermal efficiency. In addition, the high-temperature exhaust gas produced by high-temperature fuel cell can be used as an additional heat source for other purposes [4].

SOFC is a promising energy conversion system for high efficiency and fuel flexibility. The stability and reliability of all-solid-state ceramic construction can be offered by SOFC [5]. High-temperature operation, up to 1000, allows more flexibility in the choice of fuels and can produce very good performance in combined-cycle applications. SOFC approach 60% electrical efficiency in the simple-cycle system and 85% total thermal efficiency in cogeneration applications.

However, SOFC maybe has a drawback according to our understanding with respect to SOFC literatures [6, 7]. When the temperature and hydrogen flow rate were changed, a great variation was produced in the output voltage, so we may design a set of interfaces to provide a constant output voltage for SOFC. As a result, a set of electronic power devices and a controller are necessary for proper control performances. Some of the power converters to interface and the efficiency of the SOFC stack with utility are needed. The power converters are formed with a boost converter. The boost converter achieves higher voltages and smooth DC link using sliding mode control in this paper.

The paper is organized as follows. In Section 2, a model of SOFC is presented. In Section 3, a boost converter state model is introduced. Next, in Section 4, sliding mode control is designed. Finally in Section 5, the system is simulated. The conclusions are given in Section 6.

2. SOFC electrochemical model

The effects of all kinds of over potential on SOFC characteristic are considered in the electrochemical model, including heat loss and the electrical energy produced. The voltage of a SOFC can be defined as [8]:

$$(1) \quad V_{FC} = E - V_{act} - V_{ohm} - V_{conc},$$

where E is the N_{ernst} reversible voltage; V_{act} is the activation loss; V_{conc} is the concentration loss; V_{ohm} is the ohmic loss.

In the formula above, E can be calculated by Nernst equation:

$$(2) \quad E = E_0 + \frac{RT}{4F} \ln \left[\frac{(p_{H_2, ch})^2 p_{O_2, ch}}{(p_{H_2O, ch})^2} \right],$$

where $E_0 = 1.1$ V is the standard potential; R is the gas constant, 8.3143 J/(mol·K); T is the gas temperature (K); F is Faraday constant, 96485.3399 C/mol; $p_{H_2, ch}$, $p_{O_2, ch}$ and $p_{H_2O, ch}$ are the effective gas partial pressures in the channel for hydrogen, oxygen and water, respectively [9].

1) Activation voltage drop

Usually, the activation voltage drop is calculated by Butler-Volmer equation.

$$(3) \quad I = I_0 \left\{ \exp\left(\beta \frac{n_e F V_{\text{act}}}{RT}\right) - \exp\left[-(1-\beta) \frac{n_e F V_{\text{act}}}{RT}\right] \right\},$$

where $n_e=2$ is the number of moles of electrons transferred; β is the transfer coefficient and I_0 is apparent exchange current; the transfer coefficient is thought to be the fraction of the variation in polarization that leads to a variation in the reaction rate constant. Its value is 0.5 in the context of a SOFC [10]. Hence,

$$(4) \quad V_{\text{act}} = \frac{2RT}{n_e F} \sinh^{-1}\left(\frac{I}{2I_0}\right).$$

Then, the activation resistance can be defined as:

$$(5) \quad R_{\text{act}} = \frac{V_{\text{act}}}{I} = \frac{2RT}{n_e F I} \sinh^{-1}\left(\frac{I}{2I_0}\right).$$

2) Ohmic voltage drop

Ohmic overpotential, provided by the electrolyte, electrodes and interconnector of SOFC, occurs because of the resistance to the flow of ions in the ionic conductors and the resistance to electrons through the electronic conductors. Since these resistances comply with ohmic law, the overall ohmic overpotential can be shown explicitly [10]:

$$(6) \quad V_{\text{ohm}} = \left\{ \gamma \exp\left[\beta \left(\frac{1}{T_0} - \frac{1}{T}\right)\right] \right\} I,$$

where $T_0 = 973$ K, $\gamma = 0.2 \Omega$, and $\beta = -2870$ K are the constant coefficients of SOFC.

3) Concentration voltage drop

To overcome the heavy reliance on correlation to determine the limiting current density, the complete concentration over-potential equations derived in a previous research can be used, namely,

$$(7) \quad V_{\text{conc}} = \frac{RT}{4F} \left\{ \ln \left[\frac{(p_{\text{H}_2, \text{ch}})^2 p_{\text{O}_2, \text{ch}}}{(p_{\text{H}_2\text{O}, \text{ch}})^2} \right] - \ln \left[\frac{(p_{\text{H}_2, \text{ch}})^2 p_{\text{O}_2, \text{ch}}}{(p_{\text{H}_2\text{O}, \text{ch}})^2} \right] \right\}.$$

The equivalent resistance for the concentration voltage drop can be written as:

$$(8) \quad R_{\text{conc}} = \frac{V_{\text{conc}}}{I}.$$

3. Boost converter state model

It is illustrated in Fig. 1 for a circuit model of SOFC and a boost converter with a resistive load. When $K=0$, the differential equation can be calculated as [11, 12]:

$$(9) \quad \dot{I}_{L_1} = \frac{V_{\text{FC}}}{L} - \frac{V_o}{L},$$

$$(10) \quad \dot{V}_{O_1} = \frac{I_L}{C} - \frac{V_o}{R_L C}.$$

If $K=1$, the differential equation can be achieved from:

$$(11) \quad \dot{I}_{L_2} = \frac{V_{FC}}{L},$$

$$(12) \quad \dot{V}_{O_2} = -\frac{V_o}{R_L C}.$$

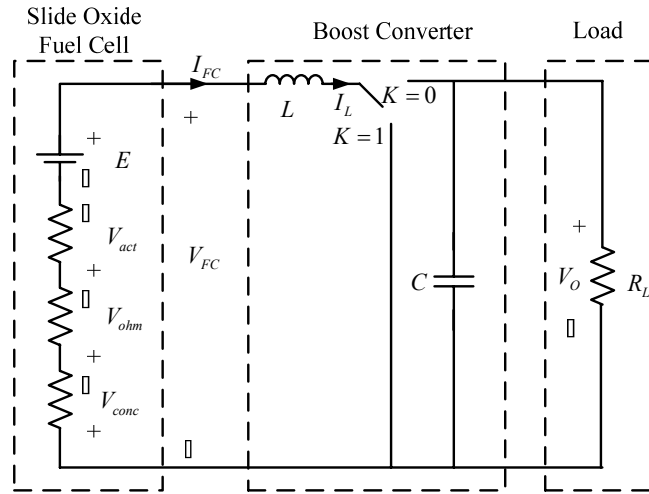


Fig. 1. Circuit model of the fuel cell and boost converter

Based on the idea of Pulse Width Modulation (PWM), the ratio of the switch in a period is expressed as a duty cycle. The dynamics of both converter configurations can be combined into a single state equation [13],

$$(13) \quad \dot{I}_L = -(1-u)\frac{V_o}{L} + \frac{V_{FC}}{L},$$

$$(14) \quad \dot{V}_o = (1-u)\frac{I_L}{C} - \frac{V_o}{R_L C},$$

where u is the duty cycle and $u \in [0 \ 1]$; C is the capacity; L is the inductance; R_L is the resistive load. Noting that the equal series resistance of the inductor and wiring resistance are ignored in the case, I_L is assumed to be equal to SOFC current (I_{FC}). In the state equation, let $x_1 = I_L$ and $x_2 = V_o$, Equations (13) and (14) can be written as:

$$(15) \quad \dot{x}_1 = -(1-u)\frac{x_2}{L} + \frac{V_{FC}}{L},$$

$$(16) \quad \dot{x}_2 = (1-u)\frac{x_1}{C} - \frac{x_2}{R_L C}.$$

The above equations can be formed as $\dot{x} = Ax + Bu$,

$$(17) \quad \begin{bmatrix} \dot{x}_1 \\ \dot{x}_2 \end{bmatrix} = \begin{bmatrix} 0 & -(1-u)\frac{1}{L} \\ (1-u)\frac{1}{C} & -\frac{1}{R_L C} \end{bmatrix} \begin{bmatrix} x_1 \\ x_2 \end{bmatrix} + \begin{bmatrix} \frac{1}{L} \\ 0 \end{bmatrix} V_{FC}.$$

4. Sliding mode control

4.1. Cascaded control structure

As can be seen in Fig. 2, the control problem can be achieved by using two structures from the cascade control circle: an inner current control loop and an outer voltage control loop. The current control is carried out by using PWM control.

Thus, the sliding mode approach is used for control of the inductor current. The block diagram of the proposed sliding mode control design is shown in Fig. 2. The command current is compared with the actual current of a sliding mode controller. The output voltage of DC/DC is controlled by a duty cycle.

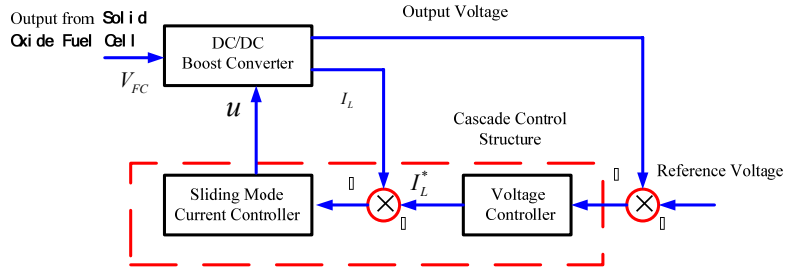


Fig. 2. Block diagram of the sliding mode control design for boost converter

4.2. Sliding mode algorithm

The state space equation 17 can be rewritten as

$$(18) \quad \dot{x}(t) = f(x, t, u),$$

where x is the state vector, u is the control input signal vector, and f is a function vector. In the sliding mode theory, if the function vector is discontinuous on a sliding mode surface, then

$$(19) \quad f(x, t, u) = \begin{cases} f^+(x, t, u^+), & s > 0, \\ f^-(x, t, u^-), & s < 0. \end{cases}$$

The aim of control is to acquire a constant output voltage denoted by V_o . In other words, the steady state conduct of the boost converter must be given by:

$$(20) \quad V_o = V_d,$$

$$(21) \quad \dot{V}_o = \dot{V}_d = 0,$$

where V_d is the desired output capacitor voltage. The control plan guarantees a two step procedure known as integrator backstepping. First, it is assumed that I_L in Equation 14 can be coped with a control input. However, because I_L is the output of

the current loop in (13), the first design step produces the desired current (I_L^*). The control objective in (21) is substituted into the voltage loop, i.e., equations (13) and (14) to produce the desired current:

$$(22) \quad I_L^* = \frac{V_d^2}{R_L \times V_{FC}}.$$

The goal of the second plan step is to assure that the actual current (I_L) tracks the desired current in (22) precisely. Because of its exact tracking properties, the sliding mode method is an ideal tool for this work. Let the state variable error be zero. It can be defined by the difference to the desired current value.

$$(23) \quad s = I_L - I_L^* = 0.$$

Then, $I_L^* = \frac{V_d^2}{R_L \times V_{FC}}$ enforces a sliding mode in the manifold $s = 0$. The control of u can be given by

$$(24) \quad u = \frac{1}{2}[1 - \text{sign}(s)].$$

Under the above control scheme, the identical control (u) comes from the Results of solving $\dot{s} = \dot{I}_L = 0$ for the control input (u), which can be obtained from (13) and (14),

$$(25) \quad u_{\text{eq}} = 1 - \frac{V_{FC}}{V_o},$$

where V_o is the output voltage of the slow voltage loop. During the sliding mode of the inner current loop, the motion equation of the outer voltage loop can be achieved from (25) and (14),

$$(26) \quad \dot{V}_o = -\frac{1}{R_L C} \left(V_o - \frac{V_d^2}{V_o} \right).$$

Finally, the state of the inner current loop attained the sliding manifold, i.e., converged to $s = 0$ when $t = t_h$, $I_L = I_L^* = \frac{V_d^2}{R_L \times V_{FC}}$, held for $t > t_h$ [14]. Equation

(26) can be explained clearly as

$$(27) \quad V_o(t) = \sqrt{V_d^2 + [V_o^2(t_h) - V_d^2] e^{-\frac{2}{R_L C}(t-t_h)}}.$$

The result of the above system tends exponentially to V_d . Thus, the design purpose of the control is realized.

The attraction domain of the sliding manifold $s = 0$ is found by utilizing the convergence condition $\dot{s}s < 0$ to the system equations (13) and (14), generating the result

$$(28) \quad V_o > V_{FC}, \text{ or } 0 < u_{\text{eq}} = 1 - \frac{V_{FC}}{V_o} < 1.$$

This equation implies the condition that as long as the output voltage is higher than the source voltage, the sliding mode can be implemented. This necessity is important for a boost-type DC/DC converter.

5. Simulation results

Figs 3 and 4 show the simulation results of the proposed control algorithm for the boost DC/DC converter. In the simulation, the converter parameters are selected as $V_{FC} = 40$ V, $C = 2$ μ F, $R = 30$ Ω , and $L = 60$ mH. The desired output voltage is $V_d = 80$ V. The proposed method is evaluated in two aspects: robustness to temperature and hydrogen flow rate. In each figure, two different values of the temperature and hydrogen flow rate are presented for comparison in order to show the robustness. Fig. 3 illustrates the tracking result with a step temperature input (from 975 up to 1030 K). The system maintains 80 V of the constant voltage within 0.25 s.

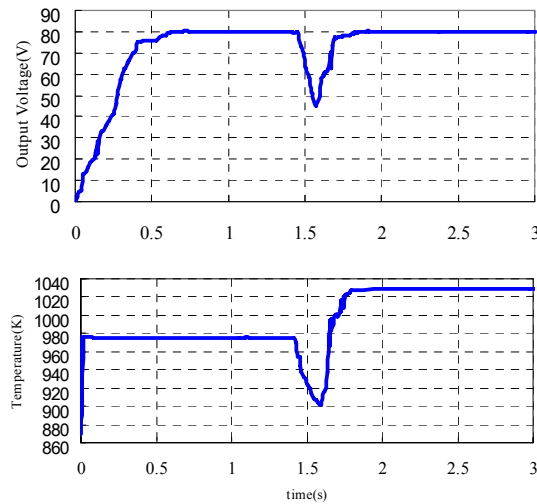


Fig. 3. Responses of the system output voltage with a temperature change

Fig. 4 shows the fuel cell system response to the hydrogen flow rate. The sliding control is tested with a sudden change of the hydrogen flow rate from 4.39×10^{-5} up to 4.47×10^{-5} . The output voltage of the system can also get a constant value. For all the results above, the sliding mode approach is able to maintain the output voltage at a constant value and robust to variety of exterior and interior conditions.

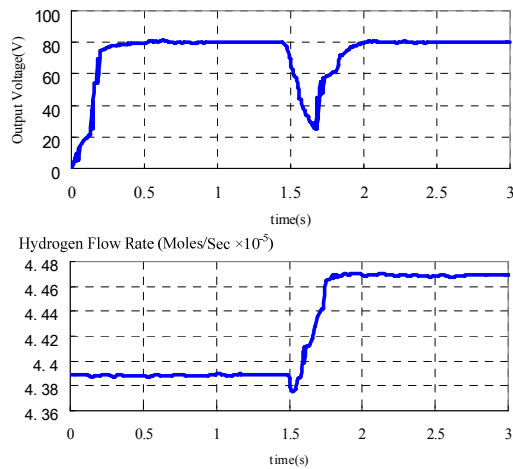


Fig. 4. Responses of the system output voltage with a hydrogen flow rate change

6. Conclusion

In this paper a sliding mode scheme which is a nonlinear control type is used to stabilize the DC voltage of the solid oxide fuel cell power generation system. The project is a promising technology that not only improves the transient response, but also reduces the steady state error of DC voltage. Furthermore, the idea of the system may be adapted to charge the battery or invert to a standard AC utility as a stand-alone system or utility-interconnected SOFC systems, which require a reliable and stable source of DC power supply.

References

1. Hart, D., G. Hormandinger. Environmental Benefits of Transport and Stationary Fuel Cells. – *Journal of Power Sources*, Vol. **71**, 1998, No 1-2, 348-353.
2. Moo, C., Y. Hsieh, I. Tsai. Charge Equalization for Series-Connected Batteries. – *IEEE Transactions on Aerospace and Electronic Systems*, Vol. **39**, 2003, No 2, 704-710.
3. Marcos, V. M., E. D. S. Gisele. A Practical Model for Evaluating the Performance of Proton Exchange Membrane Fuel Cells. – *Renewable Energy*, Vol. **34**, 2009, No 7, 1734-1741.
4. Sumi, H., R. Kishida, J. Y. Kim, H. Muroyama, T. Matsui, K. Eguchi. Correlation Between Microstructural and Electrochemical Characteristics During Redox Cycles for Ni-YSZ Anode of SOFCs. – *Journal of the Electrochemical Society*, Vol. **157**, 2010, No 12, 1747-1752.
5. Gupta, G. K., A. M. Dean, K. Ahn, R. J. Gorte. Comparison of Conversion and Deposit Formation of Ethanol and Butane Under SOFC Conditions. – *Journal of Power Sources*, Vol. **158**, 2006, No 1, 497-503.
6. Li, Y. H., S. S. Choi, S. Rajakaruna. An Analysis of the Control and Operation of a Solid Oxide Fuel Cell Power Plant in an Isolated System. – *IEEE Transactions on Energy Conversion*, Vol. **20**, 2005, No 2, 381-387.
7. Jurado, F. Predictive Control of Solid Oxide Fuel Cells Using Fuzzy Hammerstein Models. – *Journal of Power Sources*, Vol. **158**, 2006, No 1, 245-253.

8. Chan, S. H., K. A. Khor, Z. T. Xia. A Complete Polarization Model of a Solid Oxide Fuel Cell and its Sensitivity to the Change of Cell Component Thickness. – Journal of Power Sources, Vol. **93**, 2001, No 1-2, 130-140.
9. Ota, T., M. Koyama, C. Wen, K. Yamada, H. Takahashi. Object-Based Modeling of SOFC System: Dynamic Behaviour of Micro-tube SOFC. – Journal of Power Sources, Vol. **118**, 2003, No 1-2, 430-439.
10. Gebregergis, A., P. Pillay, D. Bhattacharyya, R. Rengaswemy. Solid Oxide Fuel Cell Modeling. – IEEE Transactions on Industrial Electronics, Vol. **56**, 2003, No 1, 139-148.
11. Tan, S. C., Y. M. Lai, C. K. Tse, L. Martinez Salameiro, C. K. Wu. A Fast-Response Sliding-Mode Controller for Boost-Type Converters with a Wide Range of Operating Conditions. – IEEE Transactions on Industrial Electronics, Vol. **54**, 2007, No 6, 3276-3286.
12. Sanchis, P., A. Ursæa, E. Gubia, L. Marroyo. Boost DC-AC Inverter: A New Control Strategy. – IEEE Transactions on Power Electronics, Vol. **20**, 2005, No 2, 343-353.
13. Sabzehgar, R., M. Moallem. Modeling and Control of a Boost Converter for Irregular Input Sources. – IET Power Electronics, Vol. **5**, 2012, No 6, 702-709.
14. Sira-Ramirez, H., G. Escobar, R. Ortega. On Passivity-Based Sliding Mode Control of Switched DC-to-DC Power Converters. – In: Proceedings of the 35th IEEE Conference on Decision and Control, 11-13 December 1996, Kobe, 2525-2526.